J. Astrophys. Astr. (2022) 43:49
https://doi.org/10.1007/s12036-022-09833-8

ACTIVE GALACTIC NUCLEI

Feasibility study of observing γ-ray emission from high redshift blazars using the MACE telescope

A. TOLAMATTI[1,2], K. K. SINGH[1,2,*] and K. K. YADAV[1,2]

[1]Astrophysical Sciences Division, Bhabha Atomic Research Centre, Mumbai 400085, India.
[2]Homi Bhabha National Institute, Anushaktinagar, Mumbai 400094, India.
*Corresponding author. E-mail: kksastro@barc.gov.in

MS received 27 November 2021; accepted 24 February 2022

Abstract. Blazars are the most powerful class of persistent γ-ray sources in the extragalactic Universe. Study of high redshift blazars is important to understand their cosmological evolution and formation of the supermassive black holes in the early phases of the Universe. The distant blazars are expected to be faint in the γ-ray energy band since the high-energy γ-ray photons traveling over cosmological distances are absorbed by the low-energy extragalactic background light photons via γ–γ pair production. Therefore, detection of high-energy γ-ray emission from the blazars at high redshifts using ground-based telescopes is a very challenging task. In this paper, we report the feasibility of observing high redshift blazars with the MACE gamma-ray telescope which has recently become operational at Hanle, Ladakh. We have prepared a catalog of 94 high redshift blazars from the Fourth *Fermi*-LAT catalog of γ-ray sources for their plausible observation with the MACE telescope. We have calculated the integral flux for these sources by extrapolating their *Fermi*-LAT spectra in the energy range from 30 GeV to 5 TeV. Using the MACE sensitivity information, we have estimated the total time required for the MACE telescope to detect the high-energy γ-ray emission from these high redshift blazars at 5σ statistical significance level.

Keywords. Blazars—high redshift—γ-rays—MACE telescope.

1. Introduction

Blazars, a subclass of radio-loud active galactic nuclei (AGN), are the most numerous γ-ray sources among the energetic and luminous objects in the extragalactic Universe. Their host galaxies harbor a supermassive black hole (SMBH) in the center and a pair of oppositely oriented relativistic plasma jets originating from the central region. One of the jets is in close alignment with the line of sight of the observer at Earth. These jets, considered as the manifestation of extreme astrophysical processes occurring in the central region of host galaxy, produce highly anisotropic non-thermal radiation over the entire electromagnetic spectrum ranging from radio to very-high energy (VHE; $E > 100$ GeV) γ-rays (Blandford & Znajek 1977; Urry & Padovani 1995; Blandford *et al.* 2019). The small viewing angles ($< 10^{\circ}$) of blazar jets result in the relativistic Doppler boosting of the non-thermal radiation in frequency and flux with respect to the co-moving frame of the emission region. The observed jet radiation dominates over the stellar emission from the host galaxy of the blazars and exhibits variability at different timescales from minutes to years (Aharonian *et al.* 2007; Ackermann *et al.* 2016; Singh & Meintjes 2020a). The typical broadband spectral energy distribution (SED) of blazars is described by a characteristic two-hump structure peaking at low and high energies. The origin of low-energy hump is well understood and can be attributed to the synchrotron radiation from the population of relativistic electrons in the jet magnetic field. The typical degree of polarization measured from the blazar jets in the radio and optical wavebands also supports the electron synchrotron emission in the partially ordered magnetic field (Zhang *et al.* 2015; Singh *et al.* 2019a). On the other hand, physics of the high-energy hump covering

This article is part of the Special Issue on ''Astrophysical Jets and Observational Facilities: A National Perspective''.

Published online: 12 August 2022

the γ-ray domain is not clearly known and two alternative models are proposed to explain its origin. In the widely accepted leptonic models, the high-energy component from X-ray to GeV–TeV γ-ray is described by inverse Compton scattering of low energy seed photons by the same population of relativistic electrons that produces synchrotron radiation in the blazar jet (Ghisellini *et al.* 1985; Sikora *et al.* 1994). The seed photons can be produced either inside or outside the jet depending on the location of emission region (Sikora *et al.* 2009; Singh *et al.* 2019b, 2020). In the alternative hadronic models, proton-synchrotron, photomeson and subsequent cascade of secondaries are assumed to contribute to the high-energy component of the blazar-SED (Mannheim 1993; Aharonian 2002; Cerruti 2015). Recent hints for detection of very high-energy neutrinos from the direction of blazar TXS 0506+056 during a γ-ray flaring episode provide proof of the hadronic origin of the high-energy emission from the jet (Collaboration *et al.* 2018; Zhang *et al.* 2019). Interaction of protons within the jet is followed by equipartition of their energy densities into the electromagnetic and neutrinos components and weakly interacting neutrinos escape the jet. These neutrinos carry information about the population of protons in the jet and their energy distribution function in the emission region. Therefore, multi-messenger observations are required to understand the physical processes involved in the broadband non-thermal emission from blazars.

On the basis of their observed optical properties, blazars are generally classified as flat spectrum radio quasars (FSRQ) and BL Lac (BLL) objects. The former class has optical spectra with strong emission lines and continuum of thermal contribution whereas the optical spectra of latter class are dominated by the synchrotron continuum and appear nearly featureless (Stickel *et al.* 1991; Stocke *et al.* 1991; Urry & Padovani 1995). This suggests that the host galaxy features are more prominent for FSRQs than BLLs. Therefore, redshift (z) measurements using optical spectroscopic methods are more challenging for BLLs than FSRQs (Singh *et al.* 2019). Redshift distribution of known blazars indicates that BLLs prevail over FSRQs in the low redshift range $z<0.4$ and population of FSRQs dominates at high redshifts (Ghisellini *et al.* 2017). At high z, a major fraction of extremely luminous blazars is observed to radiate in the X-ray and γ-ray energy bands. This indicates that the high redshift Universe can be probed through the observations of blazars at high z and their access to GeV–TeV energy domain would provide important information about the of evolution of blazars, propagation effects of high-energy γ-ray photons over the cosmological distances and formation of SMBHs at the early stages of the Universe (Volonteri & Stark 2011; Fabian *et al.* 2014; Sbarrato *et al.* 2015). In this work, we have performed a feasibility study for observing the probable high z blazars in the GeV–TeV regime with the recently commissioned major atmospheric Cherenkov experiment (MACE) telescope at Hanle in the UT of Ladakh, India. The manuscript is organized as following. In Section 2, we briefly discuss the high redshift blazars reported in the fourth *Fermi* gamma-ray catalog (4FGL). Methodology and source catalog for the MACE observations are described in Section 3. In Section 4, report the current status of the cosmic gamma-ray horizon due to absorption of GeV–TeV photons traveling over cosmological distances by the low-energy background photons. Finally, we conclude the study in Section 5.

2. High z blazars in *Fermi* era

The space-based γ-ray observatory, *Fermi*, launched by NASA in 2008, has revolutionised the high energy gamma-ray astronomy. The large area telescope (LAT), the primary instrument onboard the *Fermi* satellite, has opened a new energy window in the range between 30 MeV and beyond 500 GeV (Atwood *et al.* 2009). During its successful operation over a decade, the *Fermi*-LAT has increased the number of known gamma-ray sources in the sky by orders of magnitude and several successive catalog are published. In the recently released fourth *Fermi*-LAT gamma-ray source catalog (4FGL-DR2) using 10 years of data in the energy range 50 MeV–1 TeV, number of detected gamma-ray sources and their types has drastically increased over time (Abdollahi *et al.* 2020; Ballet *et al.* 2020). The population of 5788 sources reported in the above catalog has been classified into 19 types of sources and is mostly dominated by the AGNs. A total of 1920 blazars of known type (BLL:1190 and FSRQ:730) and 1515 blazars of unknown type have been identified in the 4FGL-DR2 catalog. The median and highest redshifts of blazars detected by the *Fermi*-LAT in the energy range up to 1 TeV are 1.12 and 4.31, respectively, (Ballet *et al.* 2020). The redshift distribution of BLL shows a peak at $z\sim0.3$ with a median value of 0.36 ± 0.34. Whereas, FSRQs have a redshift distribution with peak around $z\sim1$ and a median of 1.09 ± 0.68. Also, the number of FSRQs increases dramatically in the redshift range $0.5\leq z\leq2.0$ and decreases thereafter (Ajello *et al.* 2020). These distant

Fermi-LAT blazars are among the most powerful sources with soft time-averaged γ-ray spectra described by a power law with photon spectral index above ~ 2.2 and integral flux ranging from 4.8×10^{-10} to 1.5×10^{-7} ph cm^{-2} s^{-1}. The sensitivity of *Fermi*-LAT decreases significantly with increasing energy above 300 GeV. Therefore, it has become essential to observe the distant and fainter sources with soft energy spectra using ground-based γ-ray telescopes to probe the physical processes involved in the high-energy emission.

It is important to note that the 4FGL-DR2 catalog provides spectral information (shape and parameters) of sources by fitting the measured flux points in the energy range 50 MeV–1 TeV. However, the γ-ray photons of energy above a few GeV emitted from sources at $z > 0.1$ can be absorbed by the low-energy photons of the extragalactic background light (EBL) via γ–γ pair production (Gould & Schreder 1966, 1967). The absorption probability of HE photons traveling over cosmological distances is characterized by a physical quantity called optical depth (τ) or opacity. This strongly depends on the energy of γ-ray photon (E), z and density of EBL photons (Stecker *et al.* 2006; Singh *et al.* 2014). A non-zero value of τ for a given source at redshift z modifies the intrinsic γ-ray spectrum which is significantly different from the observed one (Singh & Meintjes 2020b). Figure 1 shows the estimated values of τ as a function of energy corresponding to the density of EBL photons proposed by Finke *et al.* (2010) and Dominguéz *et al.* (2011). It is evident from Figure 1 that the EBL absorption effects start dominating at energies above 30 GeV at redshift $z = 0.4$. At $z \sim 2$, the EBL absorption becomes significant for the γ-ray photons of energy ~ 10 GeV and above. Therefore, the γ-ray spectra of high redshift ($z \geq 0.4$) blazars measured by the *Fermi*-LAT in the energy range 50 MeV–1 TeV must have the imprint of the EBL absorption effects. Hence, the spectral measurements of high z blazars reported in 4FGL-DR2 catalog cannot be assumed as the representative of their intrinsic spectra.

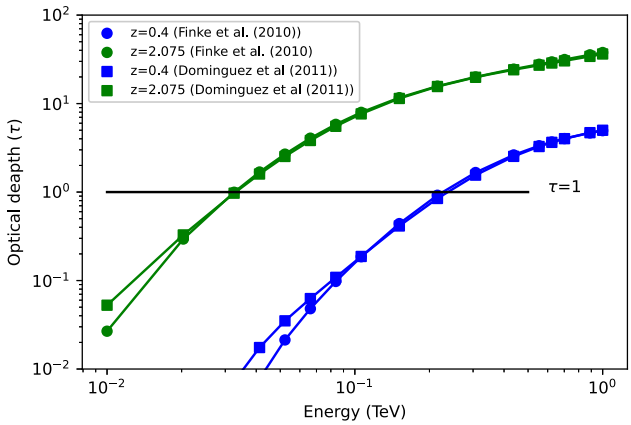

Figure 1. Optical depth values in the energy range 10 GeV–1 TeV for $z = 0.4$ and $z = 2.075$ calculated using Finke *et al.* (2010) and Dominguéz *et al.* (2011) EBL models.

3. Observations of high z blazars with MACE

Major atmospheric Cherenkov experiment (MACE) is a γ-ray telescope at Hanle (32.8° N, 78.9° E, 4270 m above sea level) in the UT of Ladakh (Koul 2017; Singh & Yadav 2021). Equipped with a 21 m diameter quasi-parabolic reflector and 1088-pixel photo-multiplier tubes based imaging camera at the focal plane, it belongs to the group of extremely large telescopes around the globe. The MACE telescope has recently been commissioned (Figure 2) and had its first light in April 2021 with successful detection of statistically significant high-energy γ-ray photons from the standard candle Crab nebula (Yadav *et al.* 2021). Monte-Carlo simulation studies for expected performance of the telescope suggest that MACE has a γ-ray trigger energy threshold of ~ 20 GeV and ~ 31 GeV for a point source with Crab Nebula like spectrum described by a simple power law and log-parabolic function, respectively (Borwankar *et al.* 2020). It has an integral sensitivity of 2.7% of the Crab Nebula flux at 5σ statistical significance level in 50 h (Sharma *et al.* 2017). The MACE telescope with a lower energy threshold and wide dynamic range of 20 GeV–5 TeV offers an excellent overlap with the energy window being explored by the *Fermi*-LAT. Therefore, MACE can be employed to observe the high redshift blazars reported in the 4FGL-DR2 catalog in the GeV–TeV energy band.

3.1 *The sample*

We have developed a detailed methodology for feasibility study of observations of high z blazars with the MACE telescope. The probable sources are first selected from the 4FGL-DR2 catalog using the following criteria:

- A source should be visible from telescope site at Hanle, i.e., its zenith angle satisfies the condition

$$Z \leq |\delta - \phi|, \quad (1)$$

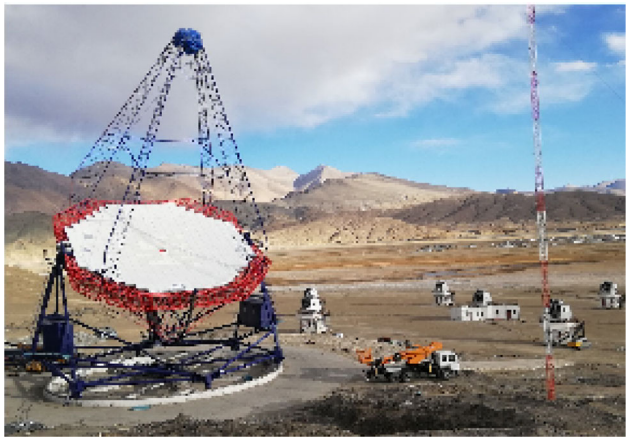

Figure 2. MACE γ-ray telescope commissioned at Hanle, Ladakh.

where δ is the source declination and $\phi = 32.8^\circ$ is the latitude of the site. MACE can be deployed to monitor the γ-ray sources up to a maximum zenith angle of 50°.

- Source should be at high redshift, i.e., $z \geq 0.4$
- The minimum value of detection significance (square root of test statistic; $\sqrt{\text{TS}}$) of a source reported in 4FGL-DR2 catalog should be 5σ (i.e., $\text{TS} \geq 25$) in the 30–300 GeV energy band. This means the sources should have significant detection by the *Fermi*-LAT over the period of 10 years in the overlapping energy range with the MACE telescope.

The selected blazars using above criteria are listed in Table 1. There are a total of 94 blazars (64 BLLs and 30 FSRQs) as plausible targets for the MACE telescope. The redshift distribution of sources identified for the MACE observations are shown in Figure 3. It is observed that most of the BLLs are concentrated in lower z whereas FSRQs are dominant at higher z. This information can be used in the study of cosmological properties like formation of SMBH and evolution of blazars, but they are beyond the scope of present work. Among the above sample of blazars, 11 have already been detected by other ground-based telescopes in the world. Results from the VHE observations of these sources are summarized in Table 2.

3.2 *Observation time*

The observational parameters of the sources (Table 1) selected for observations with the MACE telescope are estimated using the procedure described below:

- For each source, calculate the integral flux between 30 GeV and 5 TeV by extrapolating the

Table 1. List of high z blazars selected from the 4FGL-DR2 for the MACE observations.

4FGL-name	z	Class	Associated name
J0510.0+1800	0.416	FSRQ	PKS 0507+17
J0507.9+6737	0.416	BLL	1ES 0502+675
J1712.7+2932	0.420	BLL	RX J1712.8+2931
J2146.5−1344	0.420	BLL	NVSS J214637−134359
J1112.4+1751	0.421	BLL	1RXS J111224.2+175131
J0738.1+1742	0.424	BLL	PKS 0735+17
J1224.9+2122	0.434	FSRQ	4C +21.35
J1440.9+0609	0.435	BLL	PMN J1440+0610
J2055.4−0020	0.440	BLL	1RXS J205528.2−002123
J0222.6+4302	0.444	BLL	3C 66A
J1026.9+0608	0.449	BLL	NVSS J102703+060934
J2131.5−0916	0.449	BLL	RBS 1752
J1606.3+5629	0.450	BLL	RBS 1558
J1226.8−1329	0.456	BLL	PMN J1226−1328
J0227.3+0201	0.457	BLL	RX J0227.2+0201
J1756.3+5522	0.470	BLL	RX J1756.1+5522
J1109.3+2411	0.482	BLL	1ES 1106+244
J1415.5+4830	0.496	BLL	RX J1415.5+4830
J1051.4+3942	0.498	BLL	RBS 0909
J0712.7+5033	0.502	BLL	GB6 J0712+5033
J0825.8+0309	0.506	BLL	PKS 0823+033
J1032.6+3737	0.528	BLL	B3 1029+378
J0818.2+4222	0.530	BLL	S4 0814+42
J1241.8−1456	0.531	BLL	RX J1241.8−1455
J1256.1−0547	0.536	FSRQ	3C 279
J1340.5+4409	0.546	BLL	RX J1340.4+4410
J1006.5+6440	0.560	BLL	RX J1006.1+6440
J0134.5+2637	0.571	FSRQ	RX J0134.4+2638
J1101.4+4108	0.580	BLL	RX J1101.3+4108
J0114.8+1326	0.583	BLL	GB6 J0114+1325
J0238.7+2555	0.584	BLL	NVSS J023853+255407
J1642.9+3948	0.593	FSRQ	3C 345
J2022.5+7612	0.594	BLL	S5 2023+760
J2245.9+1544	0.596	BLL	87GB 224338.7+152914
J1137.9−1708	0.600	BLL	NVSS J113755−171031
J1427.0+2348	0.604	BLL	PKS 1424+240
J2345.2−1555	0.621	FSRQ	PMN J2345−1555
J0050.7−0929	0.635	BLL	PKS 0048−09
J1422.6+5801	0.635	BLL	1ES 1421+582
J0913.3+8133	0.639	BLL	1RXS J091324.6+813318
J1451.4+6355	0.650	BLL	RX J1451.4+6354
J2000.9−1748	0.652	FSRQ	PKS 1958−179
J1849.2+6705	0.657	FSRQ	S4 1849+67
J1824.1+5651	0.663	BLL	4C +56.27
J1800.6+7828	0.680	BLL	S5 1803+784
J0153.9+0823	0.681	BLL	GB6 J0154+0823
J1309.4+4305	0.691	BLL	B3 1307+433
J2321.5−1619	0.694	BLL	NVSS J232137−161935
J1517.7+6525	0.702	BLL	1H 1515+660
J0742.6+5443	0.720	FSRQ	GB6 J0742+5444
J1159.5+2914	0.729	FSRQ	Ton 599

Table 1. Continued.

4FGL-name	z	Class	Associated name
J0141.4−0928	0.730	BLL	PKS 0139−09
J1722.7+1014	0.732	FSRQ	TXS 1720+102
J1748.6+7005	0.770	BLL	S4 1749+70
J2236.3+2828	0.790	FSRQ	B2 2234+28A
J1213.0+5129	0.796	BLL	1RXS J121301.8+512942
J1533.2+3416	0.811	BLL	RX J1533.3+3416
J1037.7+5711	0.830	BLL	GB6 J1037+5711
J1151.5−1347	0.838	BLL	PMN J1151−1347
J0339.5−0146	0.850	FSRQ	PKS 0336−01
J2357.4−1718	0.850	BLL	RBS 2066
J2253.9+1609	0.859	FSRQ	3C 454.3
J1253.8+6242	0.867	BLL	1RXS J125400.1+624303
J1058.4+0133	0.890	BLL	4C +01.28
J1535.0+5320	0.890	BLL	1ES 1533+535
J0259.4+0746	0.893	FSRQ	PKS 0256+075
J0957.6+5523	0.896	FSRQ	4C +55.17
J1154.0+4037	0.925	FSRQ	B3 1151+408
J0654.4+4514	0.928	FSRQ	B3 0650+453
J1443.9+2501	0.939	FSRQ	PKS 1441+25
J0238.6+1637	0.940	BLL	PKS 0235+164
J0221.1+3556	0.944	FSRQ	B2 0218+357
J0043.8+3425	0.966	FSRQ	GB6 J0043+3426
J0433.6+2905	0.970	BLL	MG2 J043337+2905
J2232.6+1143	1.037	FSRQ	CTA 102
J1243.2+3627	1.065	BLL	Ton 116
J1146.9+3958	1.089	FSRQ	S4 1144+40
J0035.2+1514	1.090	BLL	RX J0035.2+1515
J0250.6+1712	1.100	BLL	RGB J0250+172
J0811.4+0146	1.148	BLL	OJ 014
J1048.4+7143	1.150	FSRQ	S5 1044+71
J2244.2+4057	1.171	FSRQ	TXS 2241+406
J0908.9+2311	1.184	BLL	RX J0908.9+2311
J0237.8+2848	1.206	FSRQ	4C +28.07
J1132.7+0034	1.223	BLL	PKS B1130+008
J2255.2+2411	1.370	BLL	MG3 J225517+2409
J2025.6−0735	1.388	FSRQ	PKS 2023−07
J1033.9+6050	1.401	FSRQ	S4 1030+61
J1522.1+3144	1.489	FSRQ	B2 1520+31
J1630.7+5221	1.545	BLL	TXS 1629+524
J1504.4+1029	1.839	FSRQ	PKS 1502+106
J0902.4+2051	2.055	BLL	NVSS J090226+205045
J1054.5+2211	2.055	BLL	87GB 105148.6+222705
J0323.7−0111	2.075	BLL	1RXS J032342.6−011131

spectral information provided in the 4FGL-DR2 catalog using the relation

$$F_{30\ \mathrm{GeV}-5\ \mathrm{TeV}} = \int_{30\ \mathrm{GeV}}^{5\ \mathrm{TeV}} \left(\frac{\mathrm{d}N}{\mathrm{d}E}\right)_{\mathrm{4FGL\text{-}DR2}} \mathrm{d}E, \quad (2)$$

where $(\mathrm{d}N/\mathrm{d}E)_{\mathrm{4FGL\text{-}DR2}}$ is the differential energy spectra of sources in the 4FGL-DR2 catalog. This can be described either by a simple power law or a log-parabolic function. As discussed earlier in Section 2, we have not considered the EBL attenuation effects while calculating the integral flux above 30 GeV as the measured *Fermi*-LAT spectra of blazars at $z > 0.4$ may carry imprint of the opacity of Universe to the γ-ray photons.

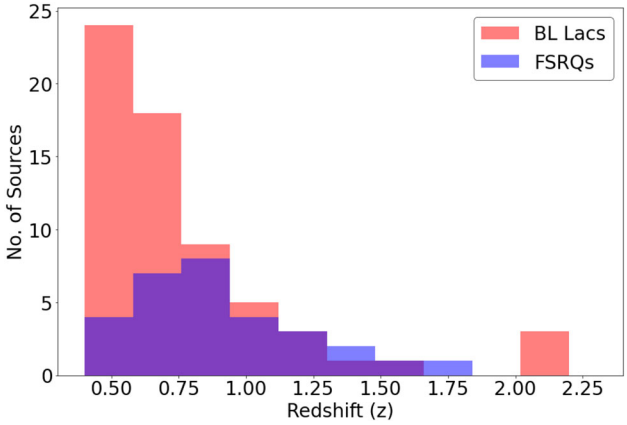

Figure 3. Redshift distribution of high z blazars visible from the MACE site.

- Convert $F_{30\ \mathrm{GeV}-5\ \mathrm{TeV}}$ to Crab units (CU) as

$$\mathrm{CU} = \frac{F_{30\ \mathrm{GeV}-5\ \mathrm{TeV}}}{F^{\mathrm{Crab}}_{30\ \mathrm{GeV}-5\ \mathrm{TeV}}}, \quad (3)$$

where $F^{\mathrm{Crab}}_{30\ \mathrm{GeV}-5\ \mathrm{TeV}}$ is the integral flux of the Crab Nebula for the MACE telescope in the energy range 30 GeV–5 TeV given in (Borwankar *et al.* 2020).

- Calculate the amount of observation time required to detect each source at 5σ statistical significance level from the sensitivity of the MACE telescope (27×10^{-3} CU in 50 h; Sharma *et al.* 2017) using the formula

$$T(\mathrm{h}) = \frac{27 \times 10^{-3}}{\mathrm{CU}} \times 50. \quad (4)$$

The distribution of integral flux estimated using Equation (2) vs. z is shown in Figure 4. We observe that the integral flux level for all the sources is of the order of 10^{-10} ph cm^{-2} s^{-1} in the dynamic energy range of MACE. This is the above the minimum detectable flux ($\sim 10^{-10}$ ph cm^{-2} s^{-1}) of the telescope. The distribution of power law spectral indices determined in the energy range 50 MeV–1 TeV from the *Fermi*-LAT measurements as a function of z is depicted in Figure 5. It is obvious that majority of the BLLs, selected for MACE observations, have hard

Table 2. Summary of high z blazars already detected by other ground-based γ-ray telescopes in the VHE band.

Associated name	z	Class	VHE-photon spectral index	Reference
4C 21.35	0.434	FSRQ	3.92 ± 0.27	Aleksić *et al.* (2011)
1ES 0033+595	0.467	BLL	3.8 ± 0.7	Aleksić *et al.* (2015)
KUV 00311−1938	0.51−0.98	BLL	5.10 ± 0.60	Abdalla *et al.* (2020)
3C 279	0.536	FSRQ	4.10 ± 0.70	MAGIC Collaboration *et al.* (2008)
PKS 1424+240	0.604	BLL	4.20 ± 0.30	Benbow (2015)
B2 1420+32	0.682	FSRQ	3.57 ± 0.29	MAGIC Collaboration *et al.* (2020)
PKS 0903−57	0.695	BLL	–	ATel 13632
TON 0599	0.729	FSRQ	~ 5	Benbow (2019)
PKS 1441+25	0.939	FSRQ	5.30 ± 0.50	Abeysekara *et al.* (2015)
B2 0218+357	0.944	FSRQ	3.80 ± 0.61	Ahnen *et al.* (2016)
PKS 0346−27	0.991	FSRQ	>4	ATel 15020

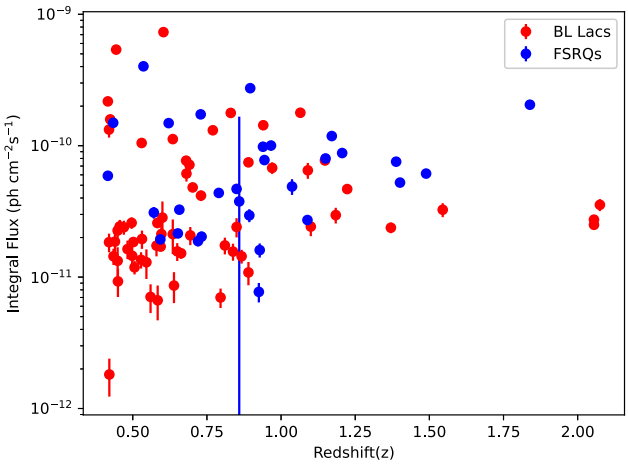

Figure 4. Integral fluxes of the selected sources in the energy range 30 GeV–5 TeV as a function of z.

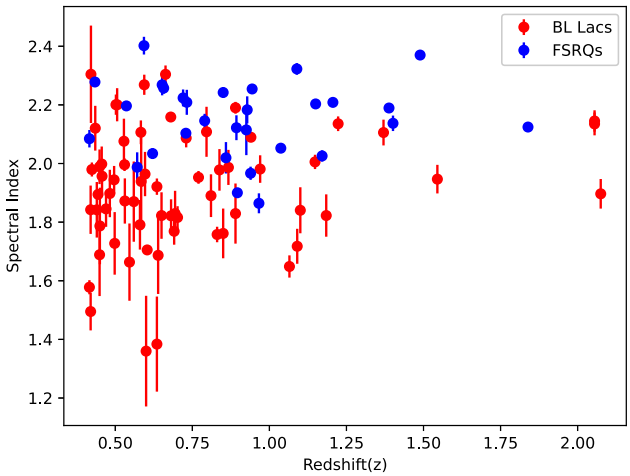

Figure 5. Power law spectral indices measured by the *Fermi*-LAT in the energy range 50 MeV–1 TeV as a function of z for sources selected for the MACE observations.

γ-ray spectra (spectral index ≤ 2) and are populated at redshifts $z < 1$. Whereas the population of FSRQs having soft γ-ray spectra (spectral index >2) is dominant at relatively higher redshifts. However, the overall *Fermi*-LAT spectral indices of the high z blazars selected for the MACE observations are harder than their VHE counterpart as reported in Table 2. Therefore, fainter high z blazar sources with soft VHE spectra can be detected with the MACE telescope. The estimated time of observation for each source at 5σ significance level is shown in Figure 6 as a function of z. It is evident that a sufficient dedicated observation time on the individual sources will be required for detecting statistically significant VHE γ-ray emission from them using the MACE telescope. However, a few well-known sources like 3C 279 and PKS 1424+240 need to be monitored for less than 5 h by the MACE telescope in order to detect VHE γ-ray emission. Therefore, such sources are the potential targets for the MACE observations of high z blazars in the beginning of its regular science program. The integral sensitivity of MACE (27 mCrab in 50 h) is better than the MAGIC-I telescope in the 20–150 GeV energy range (Sharma *et al.* 2017). Therefore, even though the current generation IACTs (H.E.S.S., MAGIC and VERITAS) have detected a number of high redshift blazars over the last 12 years, the MACE telescope will definitely enhance the detection of new high redshift VHE blazars owing to its lower energy threshold and better sensitivity in the lower energy band.

4. Cosmic γ-ray horizon

The distance (corresponding to z) traveled by a γ-ray photon of a given energy (E) for which the opacity of the Universe becomes unity (i.e., $\tau(E, z) = 1$) is

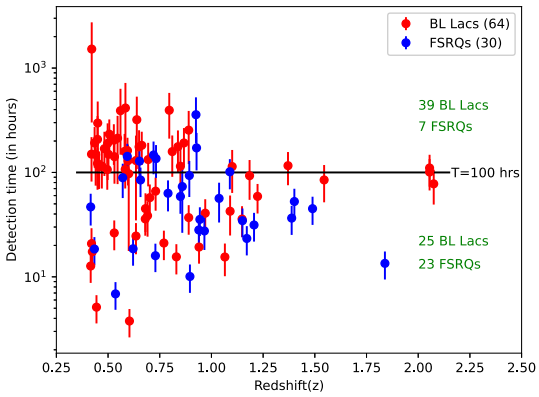

Figure 6. The distribution of estimated detection times using MACE telescope for the selected sources. 25 BL Lacs and 23 FSRQs can be detected within 100 h of observation at 5σ significance.

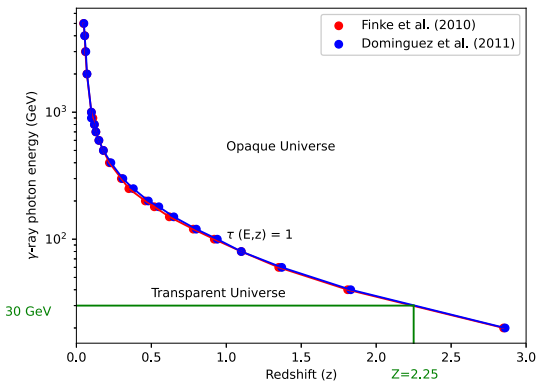

Figure 7. *Cosmic Gamma Ray Horizon* from the two famous EBL models proposed (Finke *et al.* 2010) and (Dominguéz *et al.* 2011).

referred to as the *Cosmic Gamma Ray Horizon* (Fazio & Stecker 1970). This indicates that the gamma ray horizon (GRH) corresponds to a distance traveled by a HE photon in the Universe. Thus, the Universe starts becoming opaque to the HE photons emitted from the high z blazars. The present Cosmic Gamma Ray Horizon predicted by two widely used models for the density of EBL photons (Finke *et al.* 2010; Dominguéz *et al.* 2011) is reported in Figure 7. Details of the GRH determination can be found in Singh *et al.* (2021). From the energy vs. z curve describing the GRH, it is evident that only the HE photons of energy below 100 GeV can be detected from the distant sources beyond $z \geq 1$. The MACE telescope with a lower energy threshold of $\sim$30 GeV can observe the γ-ray sources deep into the Universe up to $z \sim 2.5$. Therefore, catalog of high z blazars obtained in this study can be effectively explored by the ground-based observations with the MACE telescope to develop a better understanding of blazar physics and cosmology.

5. Summary

In this work, we present the results from a feasibility study of observing HE γ-ray emission from the high redshift blazars using the recently commissioned MACE telescope. We have prepared a list of 94 potential target sources at $z \geq 0.4$ from the 4FGL-DR2 catalog, which is based on 10 years of the *Fermi*-LAT observations. The sample consists of 64 BLLs and 30 FSRQs, with the population of BLLs and FSRQs dominating at lower and higher redshifts, respectively. We have calculated the integral flux from these sources in the MACE energy range of 30 GeV–5 TeV by extrapolating the *Fermi*-LAT spectral shape valid in energy range of 50 MeV–1 TeV. Using the MACE sensitivity information, we have estimated the amount of time required for the MACE telescope to detect these high redshift blazars at 5σ confidence level. We notice that more than half of the sources in sample list can be observed by MACE within 100 h of observation time. This study can also help in identifying other potential targets for the VHE observations with other ground-based telescopes.

Acknowledgements

The authors thank the anonymous reviewer for the critical and valuable comments that have improved the manuscript's content. Part of this work is based on archival data, software or online services provided by the Space Science Data Center – ASI.

References

Abdalla H., *et al.* 2020, Mon. Not. R. Astron. Soc., 494, 5590
Abdo A. A., *et al.* 2011, Astrophys. J., 726, 43
Abdollahi S., *et al.* 2020, Astrophys. J. Suppl., 247, 33
Abeysekara A. U., *et al.* 2015, Astrophys. J. Lett., 815, L22
Ackermann M., *et al.* 2016, Astrophys. J. Lett., 824, L20
Aharonian F. A. 2002, Mon. Not. R. Astron. Soc., 332, 215
Aharonian F., *et al.* 2007, Astrophys. J. Lett., 664, L71
Ahnen M. L., *et al.* 2016, Astron. Astrophys., 595, A98
Ajello M., *et al.* 2020, Astrophys. J., 892, 105
Aleksić J., *et al.* 2011, Astrophys. J. Lett., 730, L8
Aleksić J., *et al.* 2015, Mon. Not. R. Astron. Soc., 446, 217
Atwood W. B., *et al.* 2009, Astrophys. J., 697, 1071
Ballet J., *et al.* 2020, arxiv: 2005.11208

Benbow W. 2011, Int. Cosmic Ray Conf., 8, 51
Benbow W. 2015, Int. Cosmic Ray Conf., 34, 821
Benbow W. 2019, Int. Cosmic Ray Conf., 36, 632
Blandford R. D., Znajek R. L. 1977, Mon. Not. R. Astron. Soc., 179, 433
Blandford R. D., *et al.* 2019, Ann. Rev. Astron. Astrophys., 57, 467
Borwankar C., *et al.* 2020, Nucl. Instrum. Methods Phys. Res. A, 953, 163182
Cerruti M. 2015, Mon. Not. R. Astron. Soc., 448, 910
Domínguez A., *et al.* 2011, Mon. Not. R. Astron. Soc., 410, 2556
Fabian A. C., *et al.* 2014, Mon. Not. R. Astron. Soc., 442, L81
Fazio G. G., Stecker F. W. 1970, Nature, 226, 135
Finke J. D., *et al.* 2010, Astrophys. J., 712, 238
Ghisellini G., *et al.* 1985, Astron. Astrophys., 146, 204
Ghisellini G., *et al.* 2017, Mon. Not. R. Astron. Soc., 469, 255
Gould R. J., Schreder G. P. 1966, Phys. Rev., 16, 252
Gould R. J., Schreder G. P. 1967, Phys. Rev., 155, 1408
IceCube Collaboration *et al.* 2018, Science, 361, 1378
Koul R. 2017, Curr. Sci., 113, 691
MAGIC Collaboration *et al.* 2008, Science, 320, 1752
MAGIC Collaboration, *et al.* 2021, Astron. Astrophys., 647, 163
Mannheim K. 1993, Astron. Astrophys., 269, 67
Sbarrato T., *et al.* 2015, Mon. Not. R. Astron. Soc., 446, 2483
Sharma M., *et al.* 2017, Nucl. Instrum. Methods Phys. Res. A, 851, 125
Sikora M., *et al.* 1994, Astrophys. J., 421, 153
Sikora M., *et al.* 2009, Astrophys. J., 704, 38
Singh K. K., *et al.* 2014, New Astron., 27, 34
Singh K. K., *et al.* 2019a, Astrophys. Space Sci., 364, 88
Singh K. K., *et al.* 2019b, Mon. Not. R. Astron. Soc., 489, 5076
Singh K. K., *et al.* 2019c, Exp. Astron., 48, 297
Singh K. K., Meintjes P. J. 2020a, Astron. Nachr., 41, 713
Singh K. K., Meintjes P. J. 2020b, NRIAG J. Astron. Geophys., 9, 309
Singh K. K., *et al.* 2020, Astrophys. Space Sci., 365, 33
Singh K. K., Yadav K. K. 2021a, Universe, 7, 96
Singh K. K., *et al.* 2021b, Astrophys. Space Sci., 366, 51
Stickel M., *et al.* 1991, Astrophys. J., 374, 431
Stocke J. T., *et al.* 1991, Astrophys. J. Suppl., 76, 813
Stecker F. W., *et al.* 2006, Astrophys. J., 648, 774
Urry C. M., Padovani P. 1995, Publ. Astron. Soc. Pacific, 107, 803
Volonteri M., Stark D. P. 2011, Mon. Not. R. Astron. Soc., 417, 2085
Yadav K. K., *et al.* 2021, arxiv: 2107.04297
Zhang H., *et al.* 2015, Astrophys. J., 804, 58
Zhang H., *et al.* 2019, Astrophys. J., 876, 109